

# Future of monsoons in a changing climate – A global perspective

Joint WCRP/WWRP  
Webinar Series

## GLOBAL MONSOON

Annalisa Cherchi ([a.cherchi@isac.cnr.it](mailto:a.cherchi@isac.cnr.it))

13 September 2023

7:00-8:30 UTC



# OUTLINE

global monsoon (and its future) in IPCC AR6

monsoon projections (extremes & other  
characteristics)

decomposition of precipitation changes  
(sensitivity experiments & projections)

summary & outlook

# Global and regional monsoons in the IPCC AR6 WGI

## Global Monsoon

Ch 2: Changing state of the climate system

Ch 3: Human influence on the climate system

Ch 4: Future global climate: scenario-base projections & near-term info

## Regional monsoons

Ch 8: Water cycle changes

## Case studies, extremes, impacts (region-by-region)

Ch 10: Linking global to regional climate change

Ch 11: Weather and climate extreme events in a changing climate

Ch 12: Climate change information for regional impact and for risk assessment  
Atlas (& Interactive Atlas) for regional information

## (Summary) Monsoons box

Technical summary (Box TS.13)

## Overview/background of monsoons

Annex V

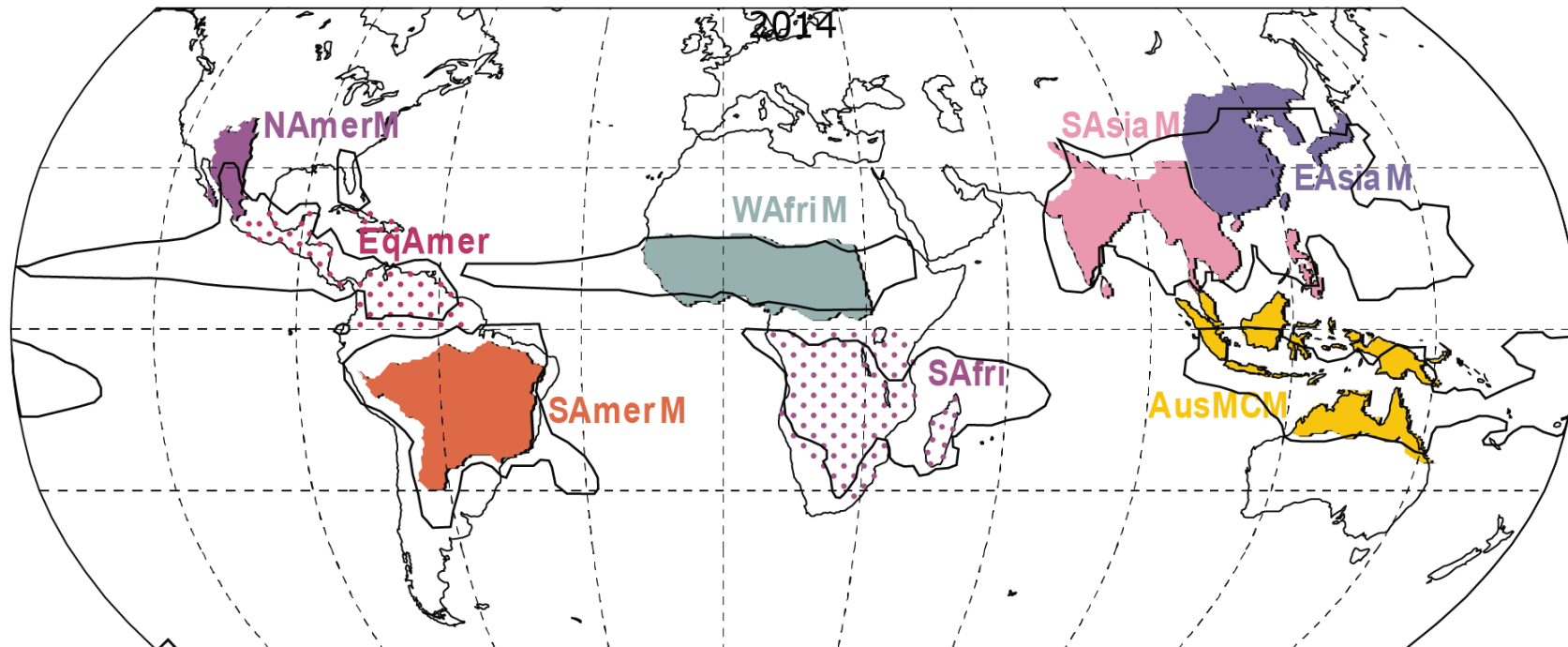
# Global and regional monsoons in the IPCC AR6 WGI



Third Lead Author Meeting of the IPCC Working Group 1  
Toulouse, August 26-30 2019



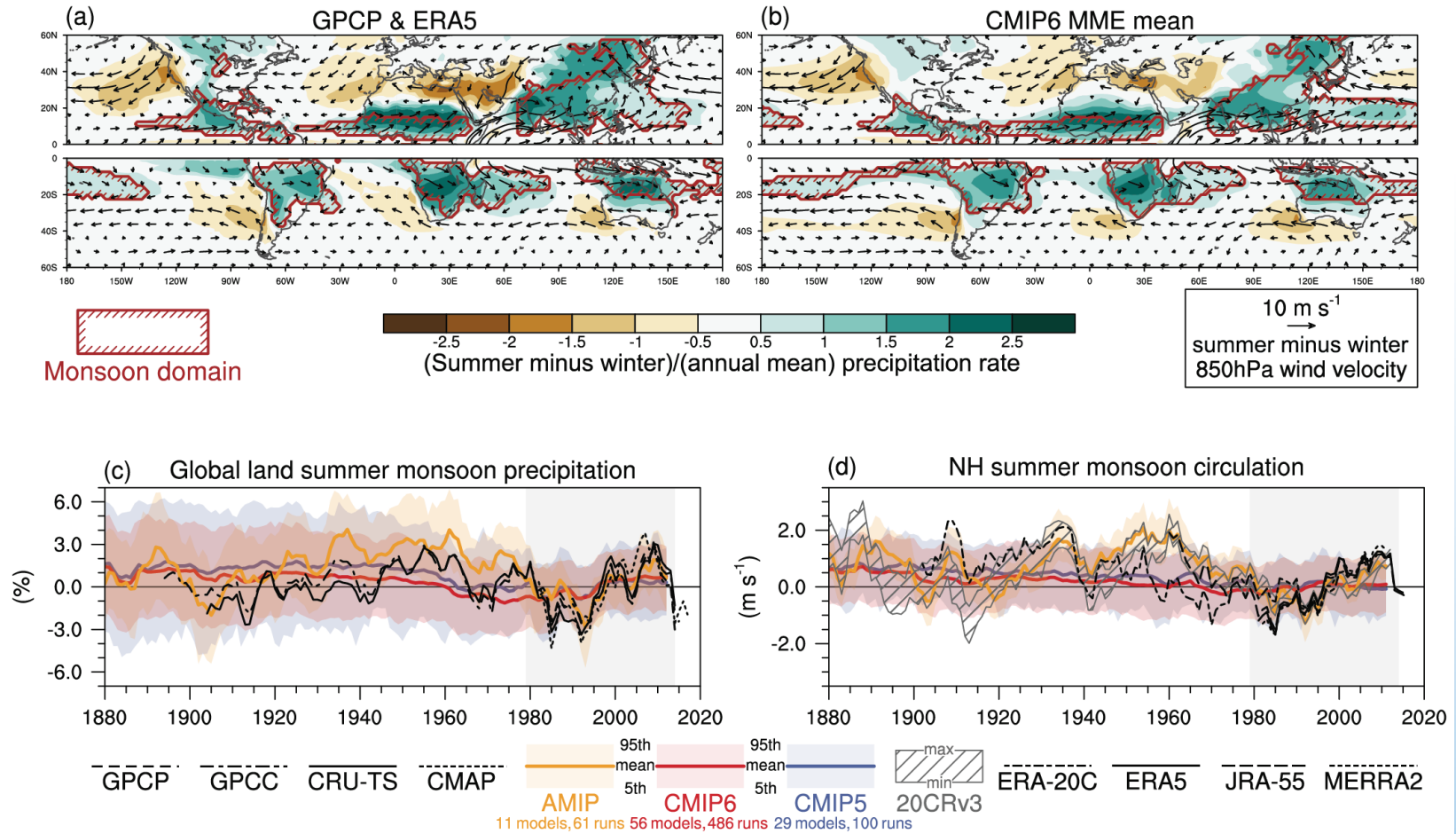
(a) Global and regional monsoon domains



Global (black contour) and regional monsoons (colour shaded) domains. The **global monsoon (GM)** is defined as the area with local summer-minus-winter precipitation rate exceeding  $2.5 \text{ mm day}^{-1}$  (see Annex V). ..... Assessed regional monsoons are South and South East Asia (*SAsiaM*, Jun–July–August–September), East Asia (*EAsiaM*, June–July–August), West Africa (*WAfriM*, June–July–August–September), North America (*NAmerM*, July–August–September), South America (*SAmerM*, December–January–February), Australia and Maritime Continent Monsoon (*AusMCM*, December–January–February). Equatorial South America (*EqSAmer*) and South Africa (*SAfri*) regions are also shown, as they receive unimodal summer seasonal rainfall although their qualification as monsoons is subject to discussion.

**Box TS.13, Fig. 1(a)**

### Global monsoon domain and intensity

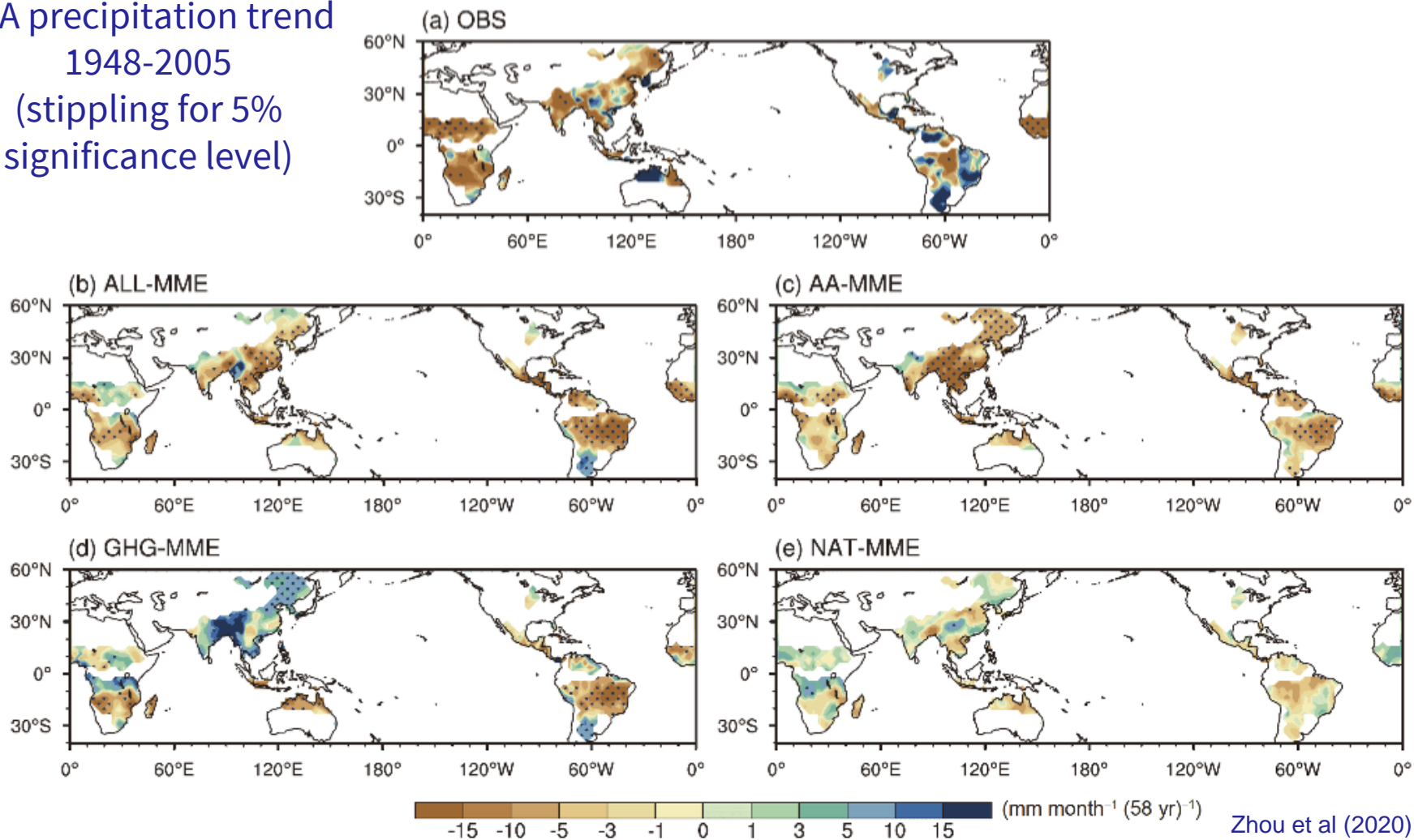


- Realistic representation of monsoon domain & precipitation intensity;
- Decline of GM precip (1950-1980) then recovery in obs & models;
- NH monsoon circulation: similar decline and then recovery

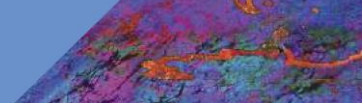
Fig. 3.17

# Attribution of monsoon precipitation changes

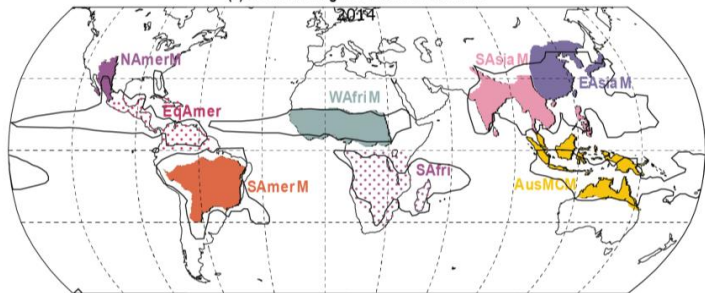
JJA precipitation trend  
1948-2005  
(stippling for 5%  
significance level)



Observed drying trend is consistent with the model simulated response to anthropogenic forcing (anthropogenic aerosol forcing) - 5 CMIP5 models results



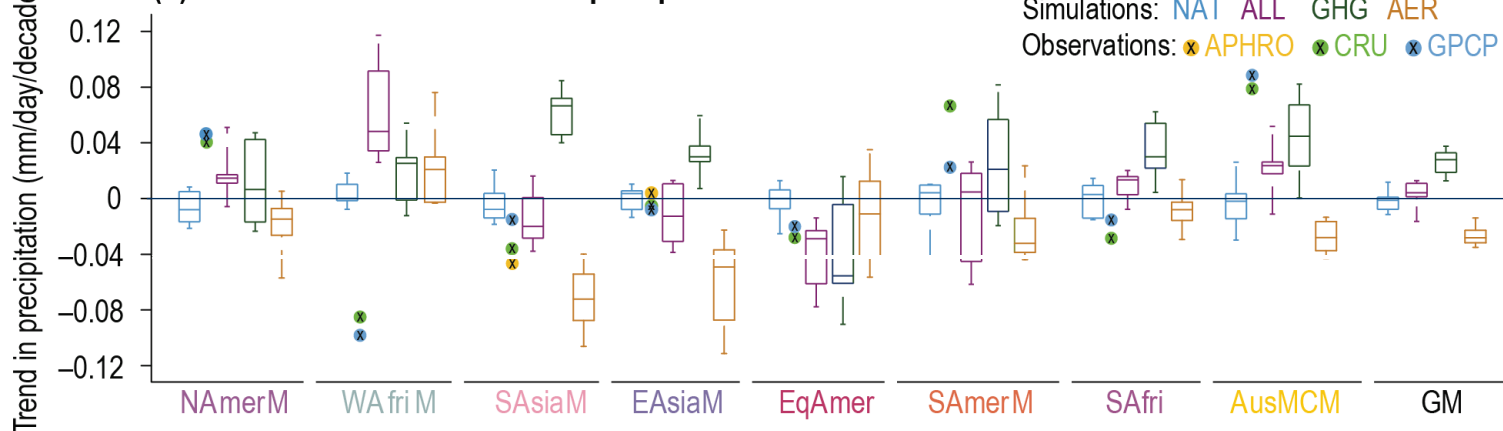
(a) Global and regional monsoon domains



# Attribution of monsoon precipitation changes

Box TS.13, Fig. 1(a,b)

(b) Historical trend in monsoon precipitation



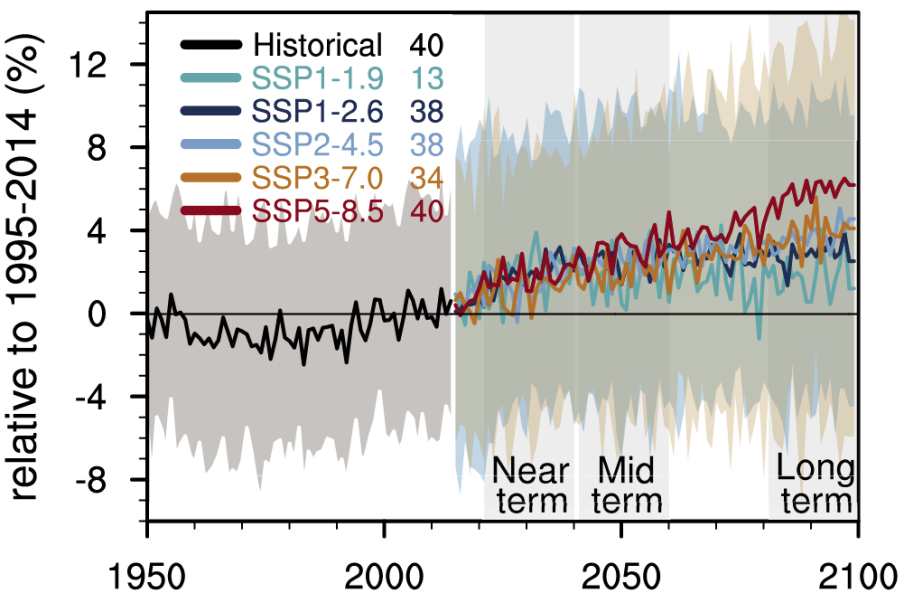
Global and regional monsoons precipitation trends based on DAMIP CMIP6 simulations with both natural and anthropogenic (ALL), greenhouse gas only (GHG), aerosols only (AER) and natural only (NAT) radiative forcing. Weighted ensemble means are based on nine Coupled model Intercomparison Project Phase 6 (CMIP6) models contributing to the MIP (with at least three members). Observed trends computed from CRU, GPCP and APHRO (only for *SAsiaM* and *EAsiaM*) datasets are shown as well.

- In the NH monsoon regions experienced declining precipitation from the 1950s to 1980s, which is partly attributable to the influence of anthropogenic aerosols (*medium confidence*). For GM the simulated change is dominated by the response of the NH monsoons (increase due to GHG balanced by decrease due to AER);
- In the instrumental records, GM precipitation intensity has *likely* increased since the 1980s, dominated by Northern Hemisphere summer trends and large multi-decadal variability.



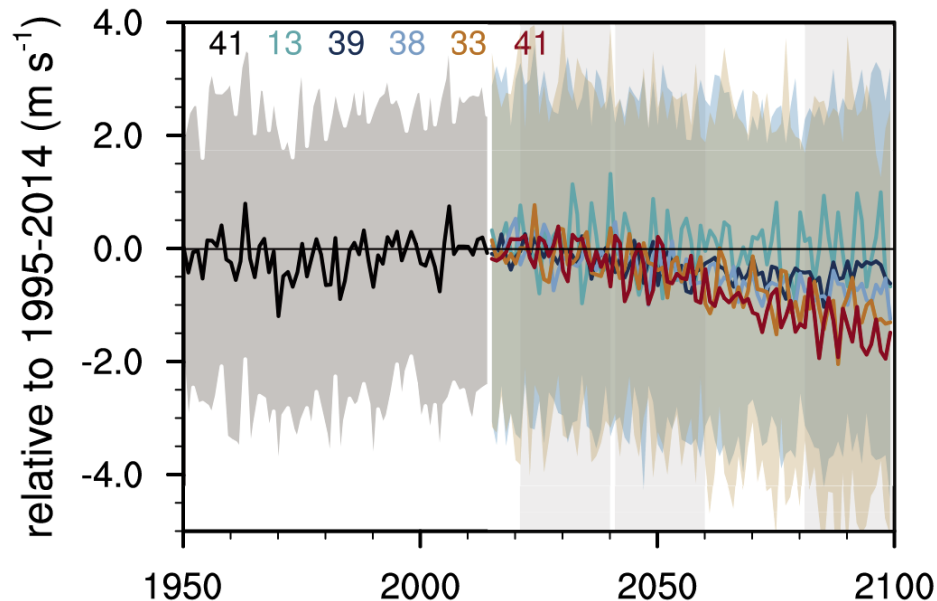
## Future changes of GM (precipitation & circulation indices)

(a) Global land monsoon precipitation index



(b) NHSM Circulation Index

Fig. 4.14



Time series of global land monsoon precipitation and Northern Hemisphere summer monsoon (NHSM) circulation index anomalies.

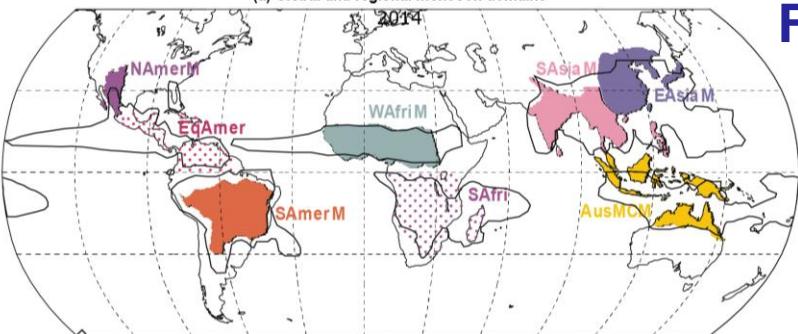
(a) Global land monsoon precipitation index anomalies (unit: %) defined as the area-weighted mean precipitation rate in the global land monsoon domain, as defined by [Wang et al. \(2013a\)](#) (b) Anomalies in NHSM circulation index (unit:  $\text{m s}^{-1}$ ), defined as the vertical shear of zonal winds between 850 and 200 hPa averaged in a zone stretching from Mexico eastward to the Philippines ( $0^{\circ}$ – $20^{\circ}\text{N}$ ,  $120^{\circ}\text{W}$ – $120^{\circ}\text{E}$ ; [Wang et al., 2013a](#)). The curves show averages over the simulations, the shadings around the SSP1-2.6 and SSP3-7.0 curves show 5–95% ranges, and the numbers near the top show the number of model simulations used.

**Near-term:** changes in GM and related circulation will be affected by the combined effects of **model uncertainty** and **internal variability** (together larger than the forced signal) – *medium confidence*;

**Long-term:** it is likely that **GM land precipitation** will increase with GSAT rise (**1.3-2.4 % increase per  $^{\circ}\text{C}$  of GSAT warming**), despite weakened monsoon circulation



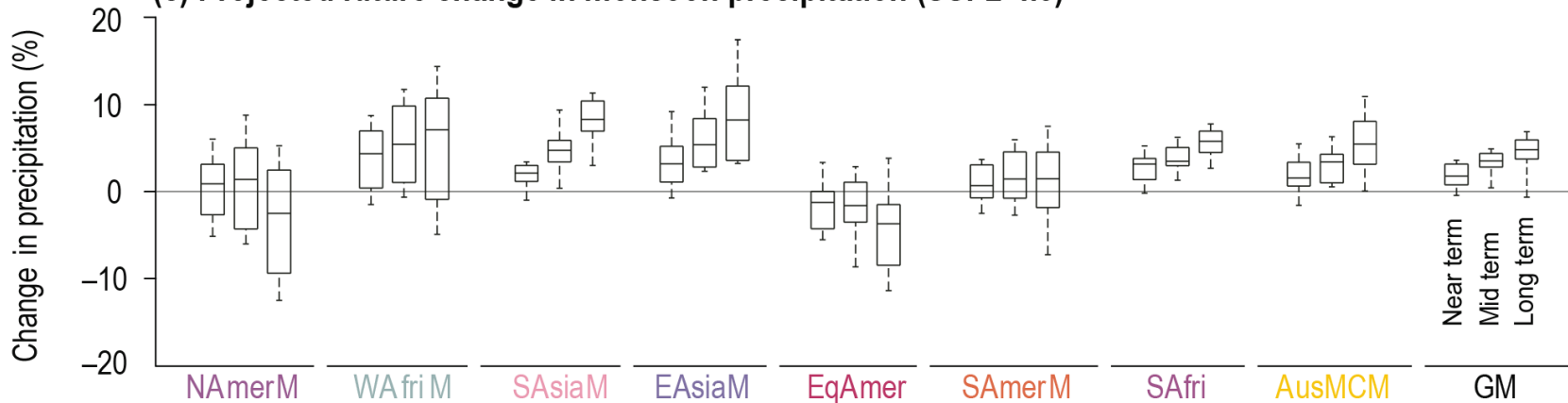
(a) Global and regional monsoon domains



# Future changes of monsoons precipitation

Box TS.13, Fig. 1(a,c)

(c) Projected future change in monsoon precipitation (SSP2-4.5)



Percentage change in projected seasonal mean precipitation over global and regional monsoons domain in the near term (2021–2040), mid-term (2041–2060), and long term (2081–2100) under SSP2-4.5 based on 24 CMIP6 models.

In the projections the increase due to GHG dominate the GM change (similarly to Asian regional monsoons – thermodynamic effects dominates)

# Decomposition of precipitation changes

## Precipitation departures

(following budget decomposition as in Chou et al., 2009)

$$P' = -\langle \bar{\omega} \partial_P q' \rangle - \langle \omega' \partial_P \bar{q} \rangle - \langle v \cdot \nabla q \rangle' + E' + q_{res}$$

q-term
ω-term
advection term
evap

Moisture terms expressed as fraction of precipitation difference

1 - P difference

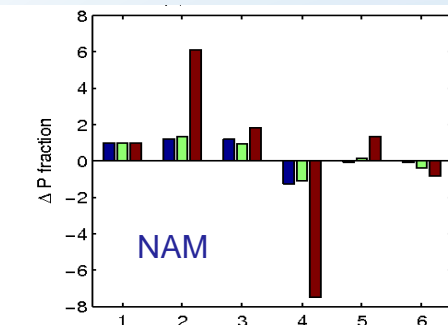
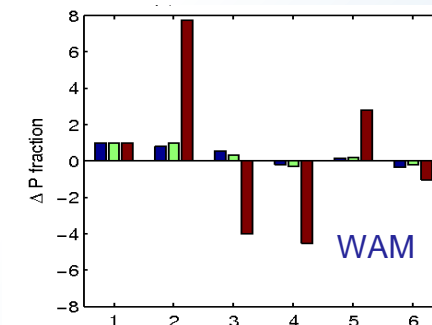
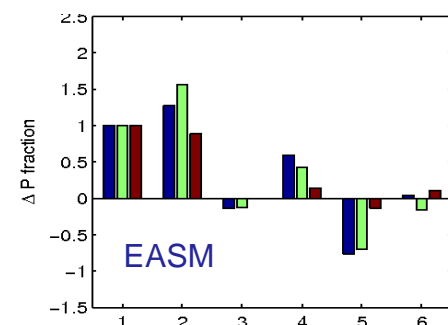
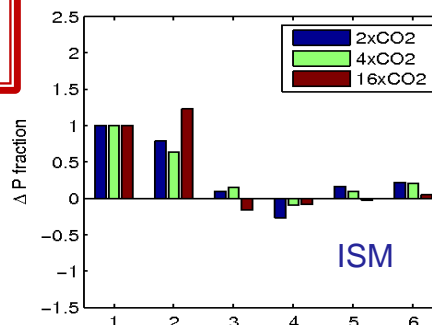
2 - q-term

3 - ω-term

4 - advection term

5 - evaporation difference

6 - residuals term (q<sub>res</sub>)

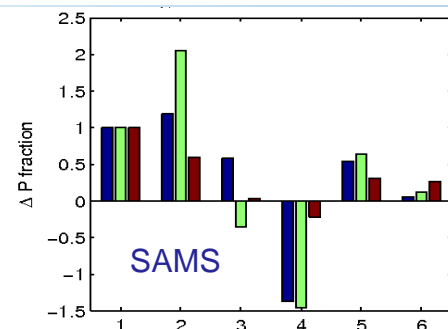
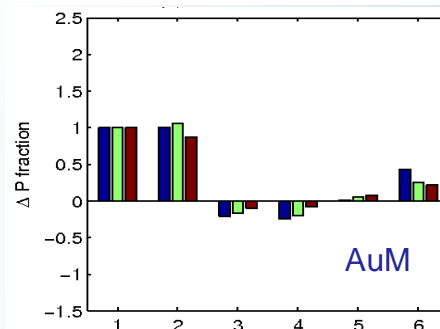


Thermodynamic component is positive, and in most cases it constitutes the largest contribution

In most cases thermodynamic contribution is damped by the other terms

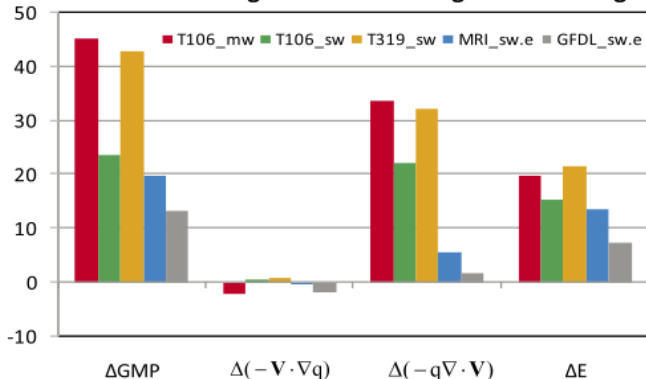
Monsoon systems may be organized into 2 categories: ISM, EASM, AuM where q-term dominates, and WAM, NAM and SAMS where ω-term and advection are equally important

WAM and NAM have a non-linear response to the forcing



# Decomposition of precipitation changes

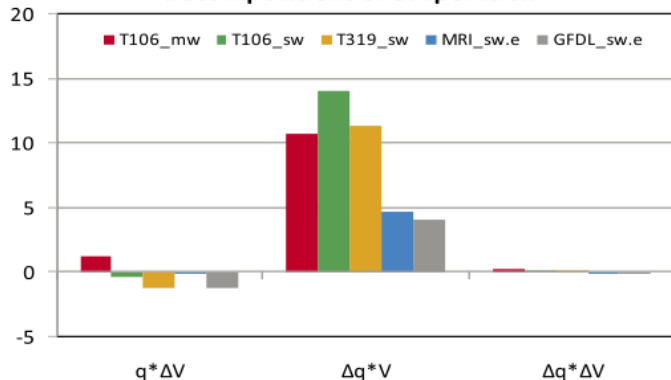
Moisture budget of GMP under global warming



Decompositions of moisture convergence



Decompositions of evaporation



| Model                          | Global Warming Experiments |   |
|--------------------------------|----------------------------|---|
|                                | Acronym                    | SST Forcing   |
| MPI ECHAM5 T106<br>(~1.125°)   | <b>T106_mw</b>             | AMIP SST in 1978–1999 plus a globally uniform SST warming (2.24°C) which is the global average of ECHAM5/MPI-OM simulated SST anomaly between A1B (2080–2100) and 20C3M (1980–2000) |
|                                | <b>T106_sw</b>             | AMIP SST in 1978–1999 plus a spatially-varying SST warming pattern derived from ECHAM5/MPI-OM simulated SST anomaly between A1B (2080–2100) and 20C3M (1980–2000)                   |
| MPI ECHAM5 T319<br>(~40 km)    | <b>T319_sw</b>             | ECHAM5/MPI-OM simulated SST in A1B (2080–2100)  |
| Japan MRI-JMA T959<br>(~20 km) | <b>MRI_sw.e</b>            | Sum of present-day (1979–2003) SST annual and interannual variations and a linear trend of future SST change derived from 18 CGCMs in CMIP3 in A1B                                  |
| US GFDL HiRAM C180<br>(~50 km) | <b>GFDL_sw.e</b>           | Future SST warming pattern [by differencing 2080–2100 (A1B) SST from the 2001–2020 SST] derived from 18 CMIP3 CGCMs was added to 1982–2005 HadISST climatology                      |

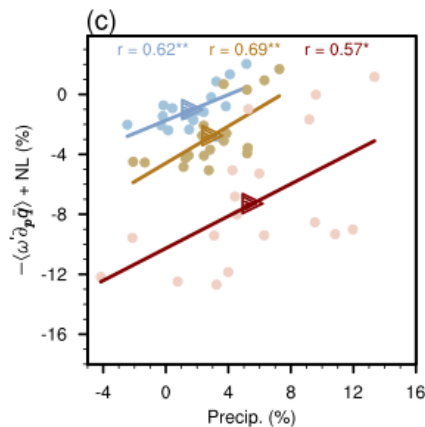
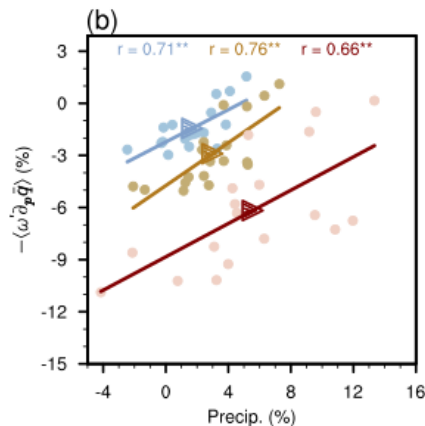
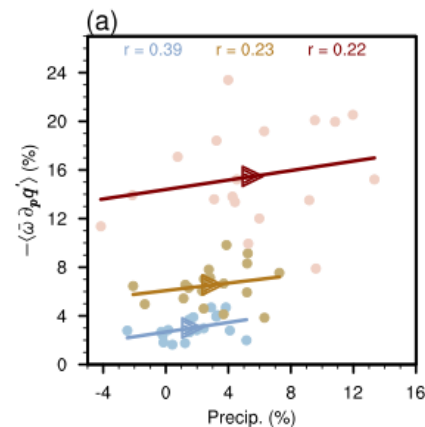
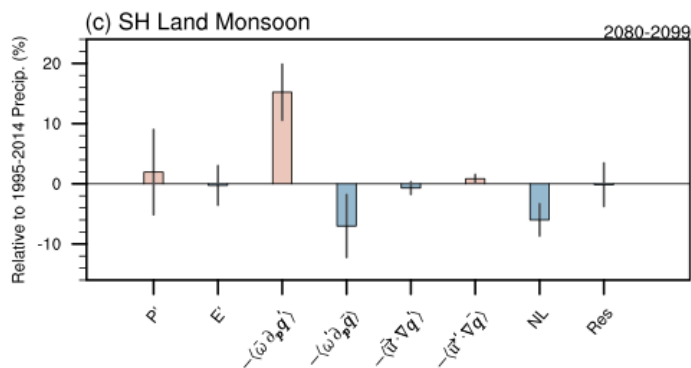
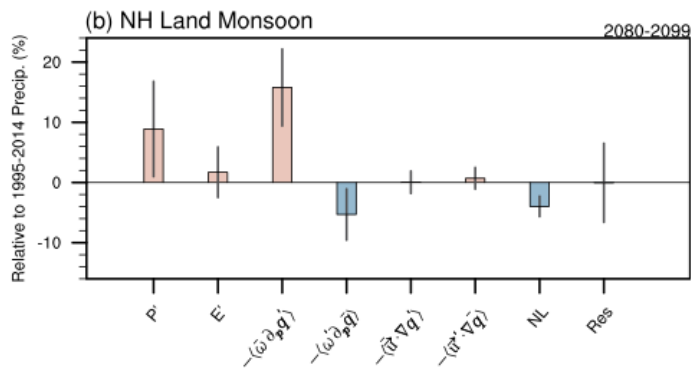
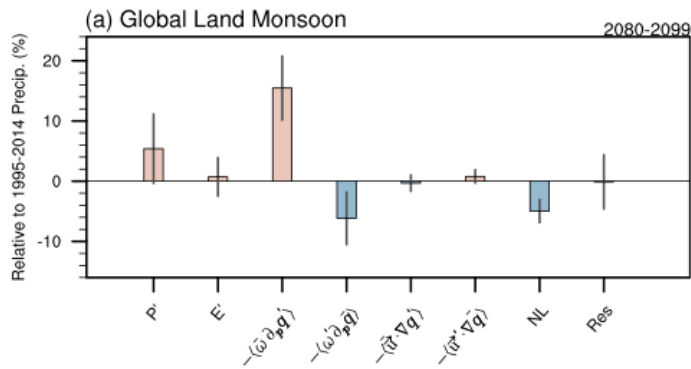
Hsu et al (2012) – GRL

the increase of the GM precipitation is attributed to the increases of moisture convergence and surface evaporation (SST prescribed experiments)

the effect of the moisture and evaporation increase is offset to a certain extent by the weakening of the monsoon circulation

similar conclusions are valid in CMIP5 models scenarios experiments (Kitoh et al, 2013)

# Decomposition of precipitation changes



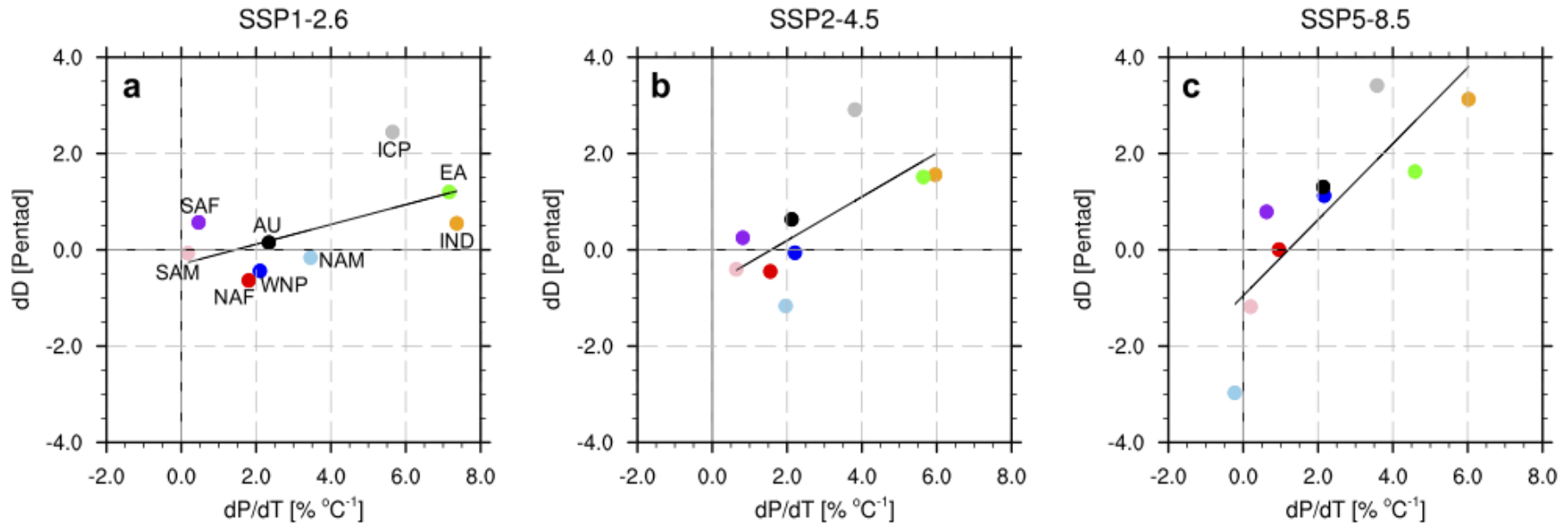
- 2080 - 2099
- ▶ MME
- 2041 - 2060
- ▶ MME
- 2021 - 2040
- ▶ MME

GLM precipitation increase caused by thermodynamic response due to increased moisture, which is partly offset by dynamic response due to weakened circulation

uncertainty in GLM precipitation projection is the largest in SSP5–8.5 scenario (in the long-term)

uncertainty of sub-monsoon precipitation projections is larger than that in GLM precipitation

# Changes in monsoons' rainy seasons: duration



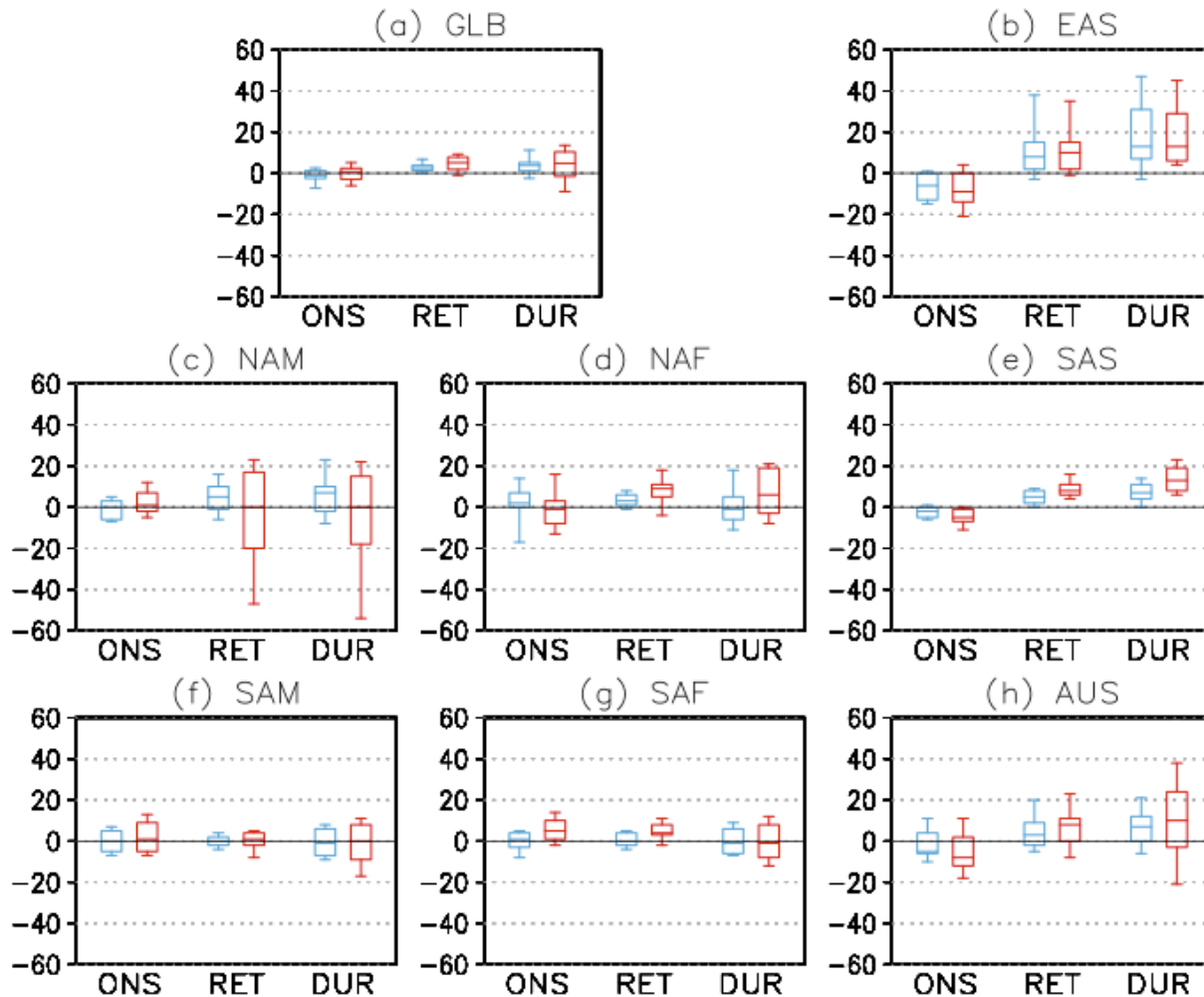
Moon and Ha (2020) – npj CAS

The duration of the rainy season has a highly positive correlation with the relative increase in the amount of precipitation per one-degree temperature increase (largest precipitation increase is associated with longer monsoon season)

Asian monsoons have the largest increase in precipitation and longest duration

American & African monsoons shortening of the monsoon rainy season

# Changes in monsoons' rainy seasons: duration, onset & retreat



Kitoh et al (2013) – JGR Atm

Onset, retreat and duration measured in days  
CMIP5 simulations (RCP4.5 in blue and RCP8.5 in red)

Monsoon retreat dates will delay

Onset dates are projected to advance (small changes)

Monsoon seasons are projected to lengthen

(largest changes in Asian monsoons, higher uncertainties in highest scenario)

# Changes in (Asian) monsoons' rainy seasons: duration, onset & retreat

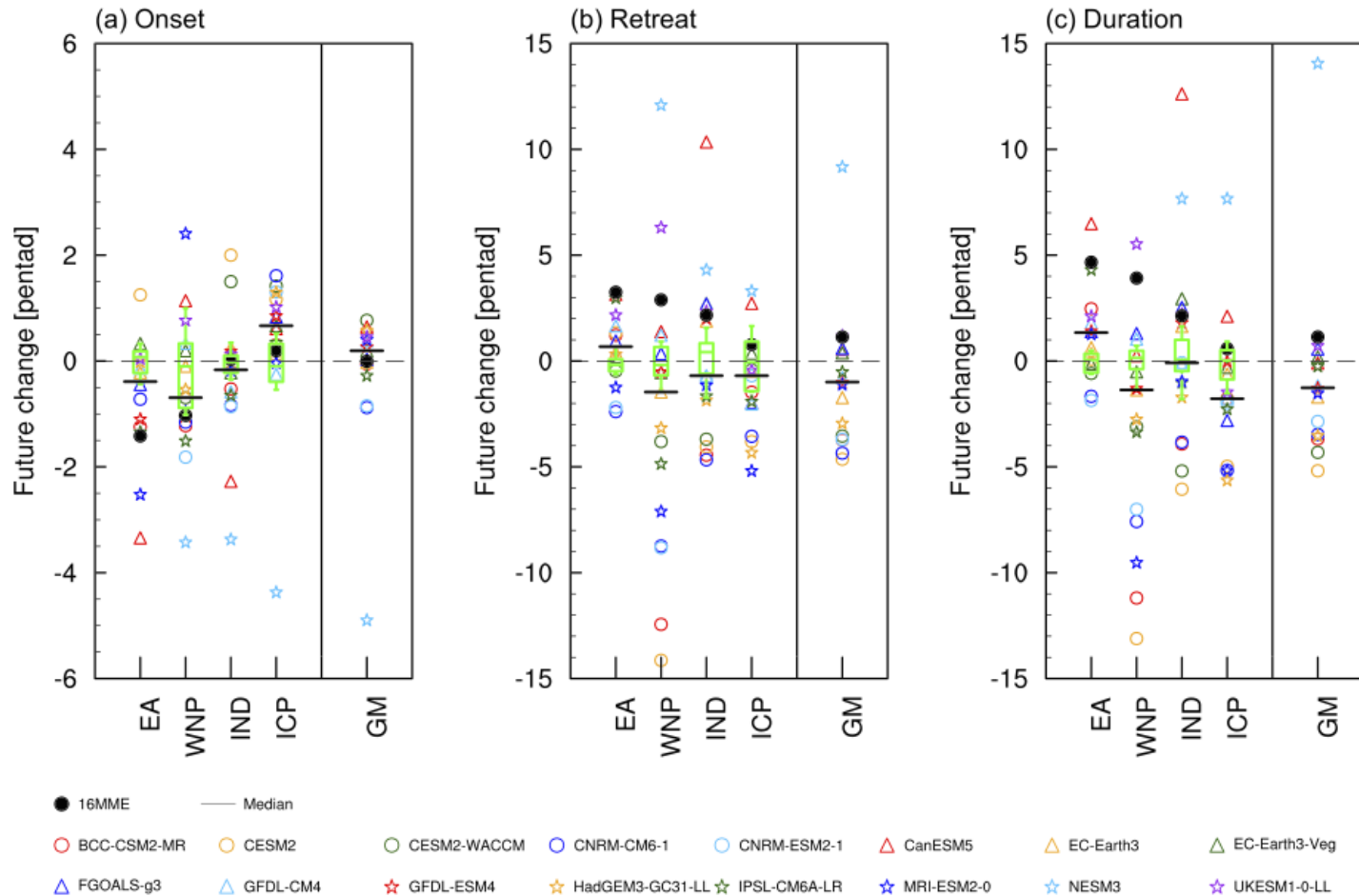


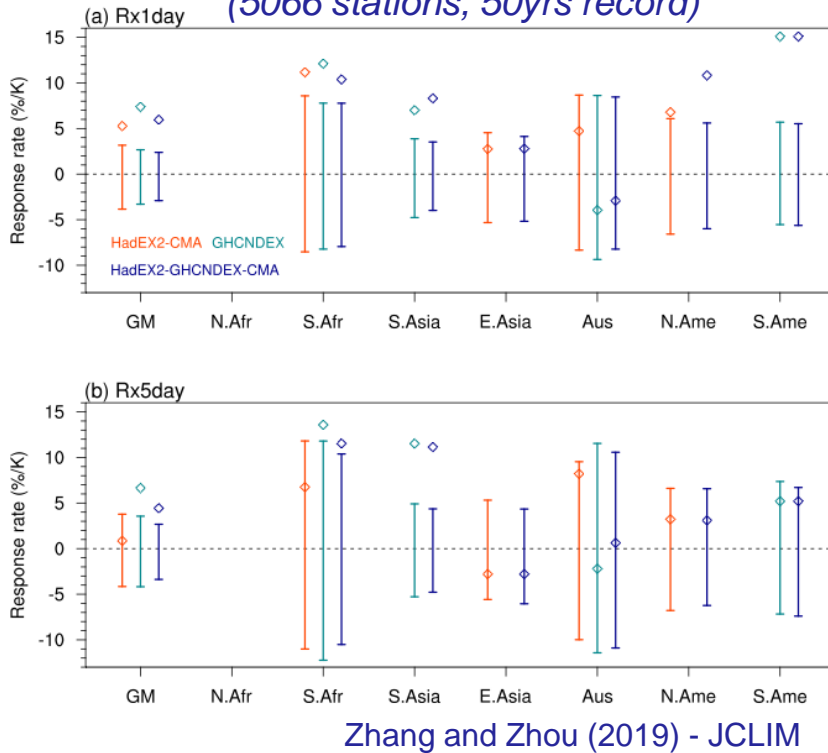
**Figure 2.** Future change (unit: pentad) in (a) onset, (b) retreat, and (c) duration of summer monsoon using CMIP6 models. The filled circle and thin line indicate the 16MME and median of 16 models changes over individual regions, respectively. The green boxes indicate the spread (from 25th and 75th quantiles, center lines indicate the median) of decadal changes based on the detrended in GPCP reanalysis from 1979 to 2014. Ha et al (2020) - GRL

- the EA will be lengthened very likely by 5 pentads due to the delayed end of monsoon season
- in the majority of Asian sub-regional monsoons, the future changes of the rainy season are larger than those over GM.

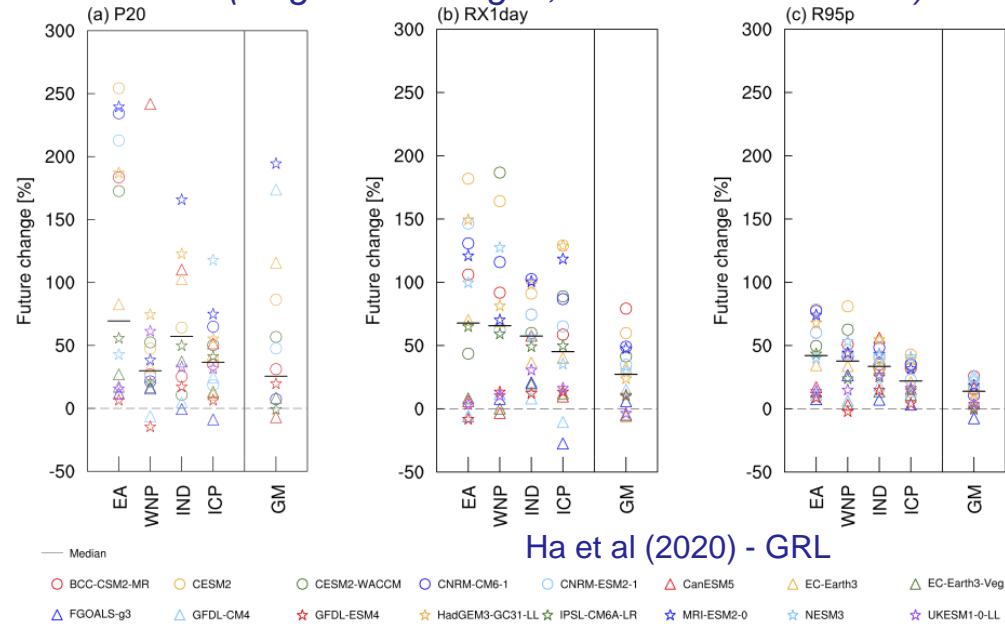


# Changes in extreme precipitation over monsoon regions

Observational extreme precipitation  
(5066 stations, 50yrs record)



CMIP6 projections (SSP2-4.5 scenario)  
(long-term changes, reference 1979-2014)



**P20** = 20-year return value of precipitation

**RX1day** = max 1-day precip

**R95p** = extremely wet day total amount (daily precip > 95<sup>th</sup> percentile of wet-day precip)

Relationship between increased mean precipitation and extreme rainfall – valid also in future projections (Jiang et al 2023)

In observed record: significant increase in annual maximum daily rainfall linked to global warming in regional monsoon domains (less robust spatial coverage for GM domain)

In models' future projections extreme rainfall events intensify (large spread)

The Asian sub-regional monsoons shows a large increasing rate of extremes in precipitation compared to GM

# Future of monsoons in a changing climate – A global perspective (summary)

- Global monsoon domain & related precipitation intensity realistically represented in state-of-the-art climate models
- Decline of GM precipitation (1950-1980) then recovery in observation & models (role of anthropogenic aerosols) – GM changes dominated by NH monsoons
- Monsoon precipitation is projected to increase in association to global warming - 1.3-2.4 % per °C of GSAT warming (despite weakened circulation) in the long-term - model uncertainty and internal variability dominate changes in the near-term;
- GLM precipitation increase caused by thermodynamic responses due to increased moisture, which is partly offset by dynamic responses due to weakened circulation – regional monsoons differences (and uncertainty)
- Longer monsoon season projected (mostly delayed retreat) but large uncertainties and regional differences
- significant increase in annual maximum daily rainfall linked to global warming in regional monsoon domains (less robust spatial coverage for GM domain) from observed records - in models' future projections extreme rainfall events intensify (large spread)

# Future of monsoons in a changing climate – A global perspective (outlook)

Identification of GM metrics in climate change perspective vs regional details (policy relevance)

Uncertainties in climate change projections (role of internal variability, differences between Asian monsoon and other regional monsoons)

Role of zonal asymmetries (AMOC, volcanoes, etc ...)

Aquaplanet framework – theoretical understanding and dynamical view (see review from Geen et al 2021 ITCZ vs monsoon)

Annalisa Cherchi (a.cherchi@isac.cnr.it)

Joint WCRP/WWRP  
Webinar Series

# GLOBAL MONSOON

13 September 2023

7:00-8:30 UTC

**THANKS FOR THE  
ATTENTION!**



# Theoretical understanding (ITCZ vs monsoon regime) – aquaplanet framework

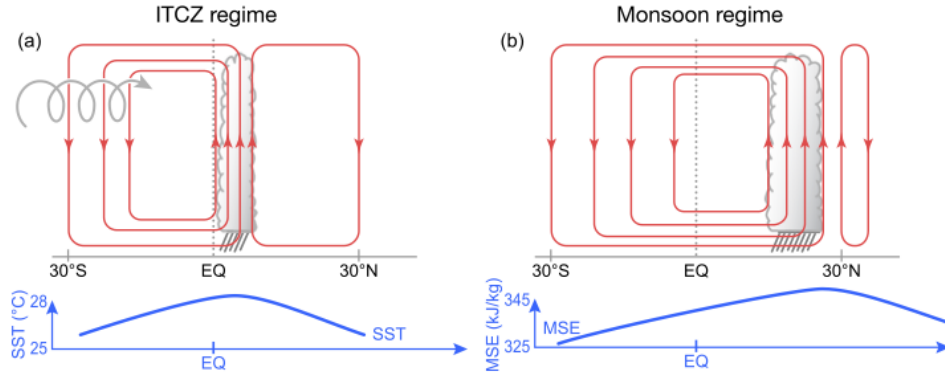


**Figure 8.** Schematic illustration of the two regimes of the meridional overturning circulation identified in aquaplanets (Bordoni & Schneider, 2008; Schneider & Bordoni, 2008). The gray cloud denotes clouds and precipitation, red contours denote streamfunction. (a) Convergence zone is an ITCZ located near to the equator, and approximately collocated with the peak SST. Hadley cells are significantly eddy driven, as indicated by the helical arrow. (b) Convergence zone is monsoon-like, located farther from the equator, with the midtropospheric zero contour of the streamfunction aligned with the MSE maximum (Privé & Plumb, 2007b) and precipitation falling just equatorward of this. The winter Hadley cell crosses the equator and is near angular-momentum conserving, with eddies only weakly influencing the overturning strength. The summer Hadley cell is comparatively weak, if present at all. Known physics of these regimes is summarized in Table 2.

Geen et al 2021 – Rev of Geophys

**Table 2**

*Suggested Classifications of Tropical and Subtropical Convergence Zones.*

| System        | Type           | Wind reversal? | Multiple preferred latitudes? | $P_{0-10^\circ}$ (%) | $P_{10-25^\circ}$ (%) | $P_{25-35^\circ}$ (%) | $\phi(\theta_{eb})$ (°) | $\phi(P_{max})$ (°) |
|---------------|----------------|----------------|-------------------------------|----------------------|-----------------------|-----------------------|-------------------------|---------------------|
| South Asia    | Monsoon        | yes            | yes                           | 24                   | 57                    | 19                    | 25                      | 21.25               |
| Australia     | Hybrid         | yes            | yes                           | 48                   | 44                    | 8                     | -7.5                    | -6.25               |
| West Africa   | Hybrid         | yes            | yes                           | 58                   | 40                    | 2                     | 12.5                    | 8.75                |
| South Africa  | Monsoon        | yes            | yes                           | 33                   | 54                    | 13                    | -12.5                   | -13.75              |
| North America | ITCZ extension | no             | no                            | 32                   | 55                    | 13                    | 10.                     | 8.75                |
| South America | Neither        | no             | yes                           | 41                   | 43                    | 16                    | -12.5                   | -6.25               |
| Atlantic      | ITCZ           | no             | no                            | 69                   | 19                    | 12                    | 2.5                     | 6.25                |
| East Pacific  | ITCZ           | no             | no                            | 50                   | 35                    | 15                    | 7.5                     | 8.75                |

*Note.* Regions are defined as in Figures 1 and 15. Wind reversal is assessed based on Figure 1, and the presence of multiple preferred latitudes for rainfall is based on Figure 15.  $P_{0-10^\circ}$ ,  $P_{10-25^\circ}$ , and  $P_{25-35^\circ}$  are the area-weighted fractions of precipitation (mm/day) falling in each monsoon/ITCZ region between the indicated latitudes (bounded in longitude by the boxes in Figure 1), relative to the total evaluated from 0–35°. Conclusions are not sensitive to small variations in the latitude bounds used; the use of 10° rather than 7° (cf. Geen et al., 2019) here is motivated by discussion in section 3.2.1.  $\phi(\theta_{eb})$  and  $\phi(P_{max})$  are the latitudes of maximum season-mean subcloud equivalent potential temperature and precipitation, respectively. Precipitation fractions and maxima are calculated using GPCP data, and  $\theta_{eb}$  is calculated using JRA-55 reanalysis, with 1979–2016 used in both cases. Season means over June–September are used for Northern Hemisphere monsoons, December–March for Southern Hemisphere monsoons, and all months for the Atlantic and Pacific ITCZs.